X-Ray Pulse Height Analysis on ASDEX Upgrade

A. Weller[1], B. Huber[1], J. Belapure[1], T. Pütterich[1], M. Sertoli[1], A. Gude[1],
R. Neu[1], R. Dux[1], W. Suttrop[1], and the ASDEX Upgrade Team

[1]*Max-Planck-Institut für Plasmaphysik, D-85748 Garching, Euratom Association, Germany*

The Soft X-ray (SX) pulse height analysis (PHA) system at the ASDEX Upgrade tokamak (AUG) was refurbished recently. The new silicon drift detector (SDD) has an active area of 8 mm^2, a thickness of 450 µm, and is supplied with an 8 µm thick Beryllium window. The operation temperature is typically at about -20° C, provided by an integrated Peltier cooler. The output signals of the new pulse reset preamplifier are processed by a commercial digital signal analyzer which allows offline energy calibration measurements as well as online time resolved spectroscopy. In order to achieve processed pulse rates of up to 500 kcps the digital filter was set up with fast rise and flattop times (0.2 µs each). The dynamic range and spectral response can be controlled by exchangeable pinholes and Beryllium foils of 2 - 1000 µm thickness, respectively. Thus, the system is sensitive to photons of > 0.5 keV in the case without additional Be-foil. The efficiency reduces gradually above 10 keV due to the finite detector thickness. A retractable X-ray tube is used for in-situ energy calibration which yields an absolute calibration of the radiated X-ray power at the same time. Actually, the PHA system has the potential for cross calibrations of the Johann- and Bragg-spectrometers as well as of the soft X-ray cameras on AUG.

Since in AUG all plasma facing components are coated with tungsten to explore fusion relevant plasma scenarios [1], the X-ray PHA spectra are typically characterized by dominant line radiation from highly ionized tungsten impurities in the energy range 1.5 - 3.1 keV (0.4 - 0.8 nm) originating from ionization stages W^{39+} - W^{47+} [2]. Since the typical energy

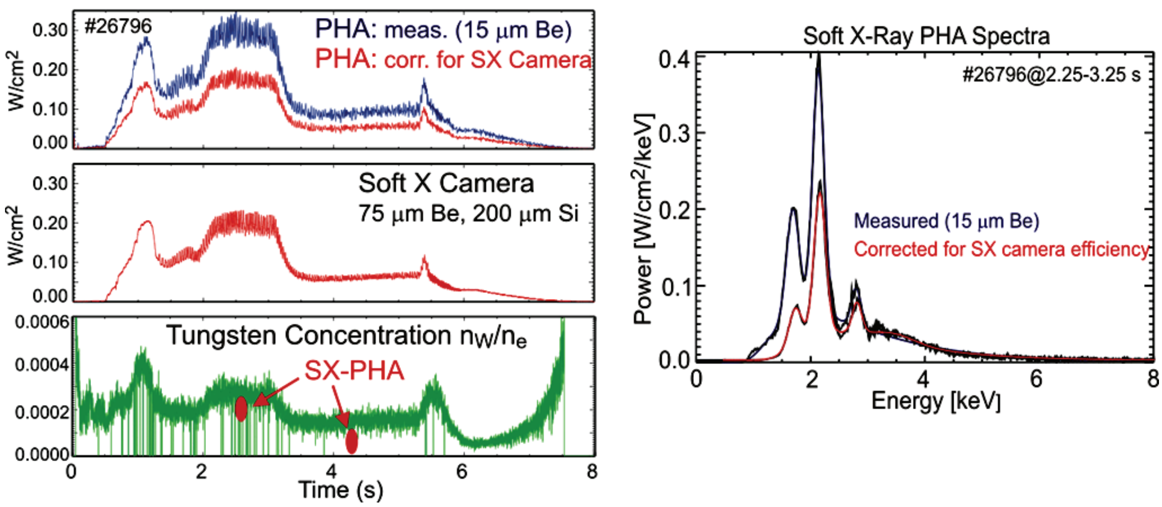

Fig. 1 Left: Energy integrated PHA signals compared with SX Camera data, and tungsten concentration from VUV spectroscopy in a low density L-mode plasma. Right: Measured tungsten line dominated PHA spectra including correction for simulating the SXC response. W concentrations are obtained using calculated coronal cooling rates and taking the SX camera efficiency into account.

resolution of the PHA system at 5.9 keV is in the range 140 - 180 eV (depending on the digital filter setting) only 3 clusters of different tungsten lines can be resolved (PHA spectrum in fig. 1, measured with 15 µm Be-filter). The smooth solid lines through the data points, which are also present in the next figures, are fits composed of a cut-off exponential describing the continuous background spectrum and of Gaussians for the line radiation. The lowest energy component centered around 1.7 keV (0.68 nm) is attributed to 4-3 transitions in W^{46+} and W^{47+} (M-lines). This feature disappears below $T_e = 1\text{-}1.5$ keV. The most prominent component around 2.15 keV (0.58 nm) originates from 4-3 transitions in $W^{38+\ldots45+}$. The center of this peak shifts down to about 1.9 keV (6.5 nm) as the central electron temperature decreases from $T_{e0} >$ 2.5 keV down to $T_{e0} \approx$ 1 keV. At least in the low temperature range inner shell ionization and/or dielectronic recombination effects are considered to contribute to this emission. Finally, the smaller peak around 2.6 keV (0.58 nm) is due to 5-3 transitions excited in $W^{38+\ldots45+}$ ions [2].

In fig. 1 time traces of the X-ray energy integrated intensities in a low density L-mode discharge measured by the PHA and the soft X-ray camera (SXC) systems are shown together with the tungsten concentration derived from the intensity of the quasi-continuum emission from W^{27+} - W^{35+} [2]. The drop at 3.1 s coincides with the time when the RMP coils [3] are switched on; all global discharge parameters remain unchanged. The PHA data allow a cross-check with the SXC data by normalizing the PHA spectra with the ratio of the different PHA and SXC spectral detection efficiencies given by the filter and active detector layer characteristics. The absolute intensities agree typically within about 15%. A typical measured PHA spectrum and its normalization to the SXC detection efficiency is shown in fig. 1 (right). Using measured T_e and n_e profiles and calculated coronal cooling rates for

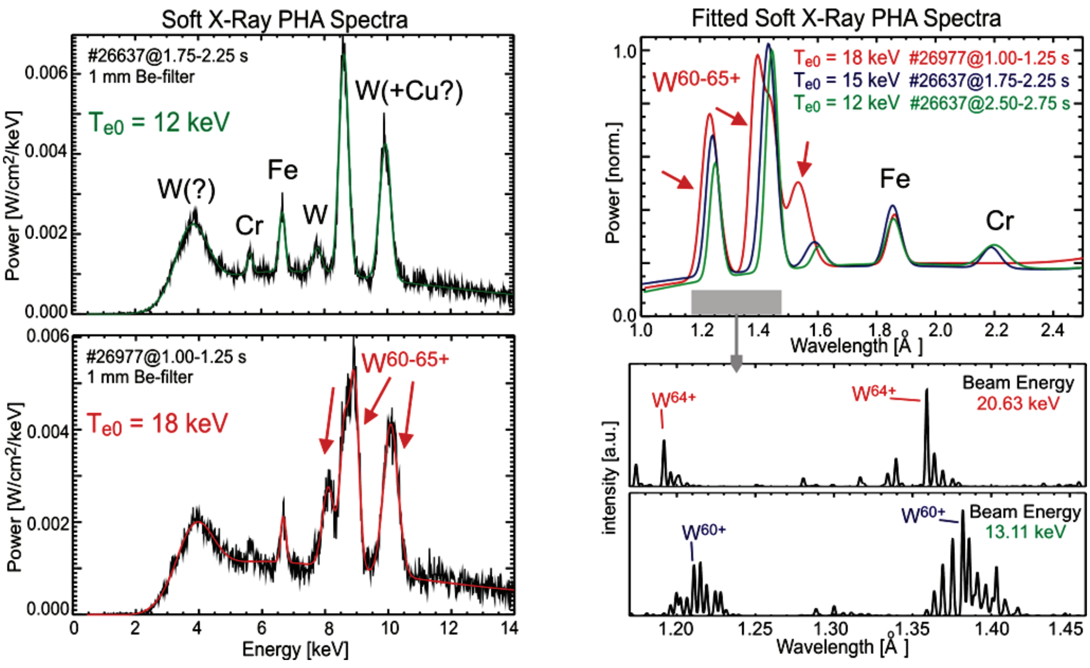

Fig. 2 Left: PHA spectra taken with 1 mm Be-filter in high-T_e discharges. Right: The appearance of high ionization stages of Tungsten in the range W^{60+} - W^{65+} is indicated. The lower part contains calculated line intensities for transitions measured at different beam energies in the EBIT device.

tungsten including the SXC response function [4], tungsten concentrations in the range $n_W/n_e = 6 \cdot 10^{-5}$-$2 \cdot 10^{-4}$ were derived from the X-ray measurements, which are slightly below the values obtained from VUV spectroscopy (fig. 1, lower left). Here, the X-ray emission was assumed to originate from tungsten solely. The relatively large concentrations are due to low density L-mode operation.

At very high temperatures (up to 18 keV) achieved with combined ECRH and NBI heating at low densities, very prominent tungsten L-line radiation (3-2) in the energy range 8.1-10.1 keV has been detected for the first time in a fusion plasma (fig. 2). It is accompanied by a cluster of lines appearing around 4 keV which are not yet classified. A 1 mm Be-filter was used to highlight the high energy part in the PHA spectra. The high energy lines are attributed to tungsten, but some masking by copper K-lines cannot be excluded, although no clear evidence of copper was found in the VUV spectra. In the upper right part, a comparison of fitted spectra obtained with different central electron temperatures is given. The same data are converted here to a wavelength scale. Actually, these lines which will be relevant in ITER have been investigated among others in the EBIT device [5],[6] and were modeled by the ADAS code package [2] (lower right). The present data, in particular the dependence on T_e, are well consistent with the appearance of ionization stages in the range W^{60+} - W^{65+}.

Apart from tungsten, a number of additional impurities including Ar, Ca, Ti, Cr, Fe and Cu are found frequently, and associated concentrations have been estimated and compared with other spectroscopic data. Whereas the tungsten influx is mainly due to sputtering at the chamber wall and the divertor target plates [7], additional effects such as arcing have to be considered to explain the influx from remote and shielded parts of the wall or in-vessel components. Argon was released sometimes after shots in which a disruption was mitigated by massive gas injection. Also, it can originate from a leaking gas filled X-ray detector.

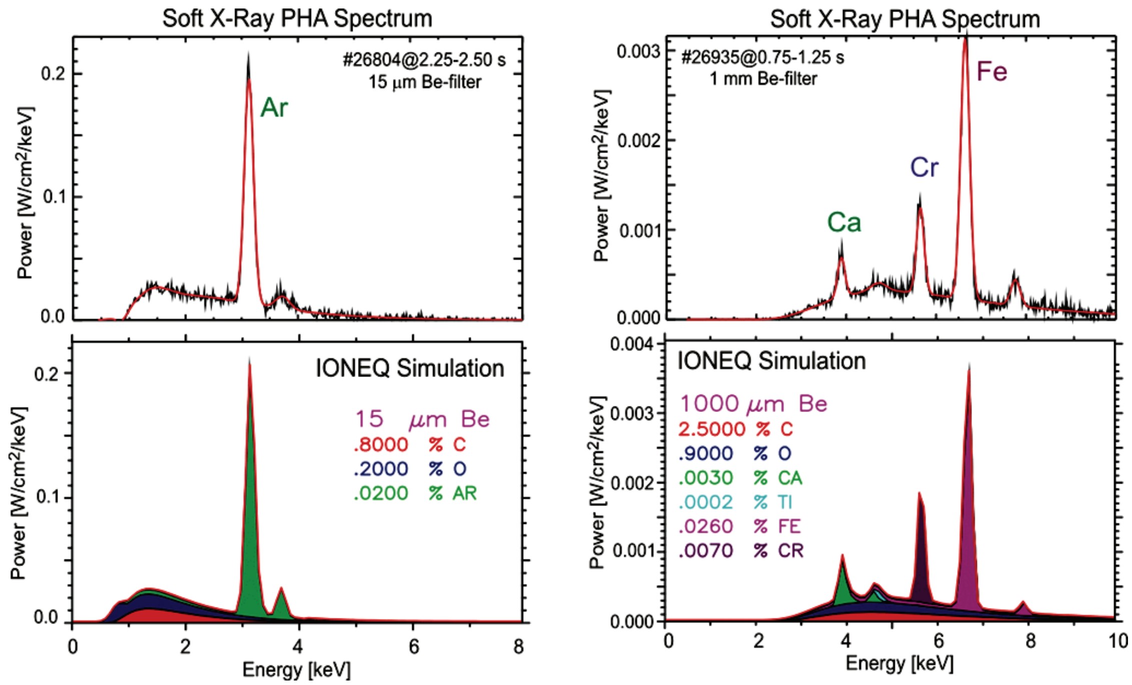

Fig. 3 Examples of X-ray PHA spectra measured with Be-filters of 15 μm (left) and 1 mm (right), respectively. Impurity concentrations are estimated by matching simulated spectra.

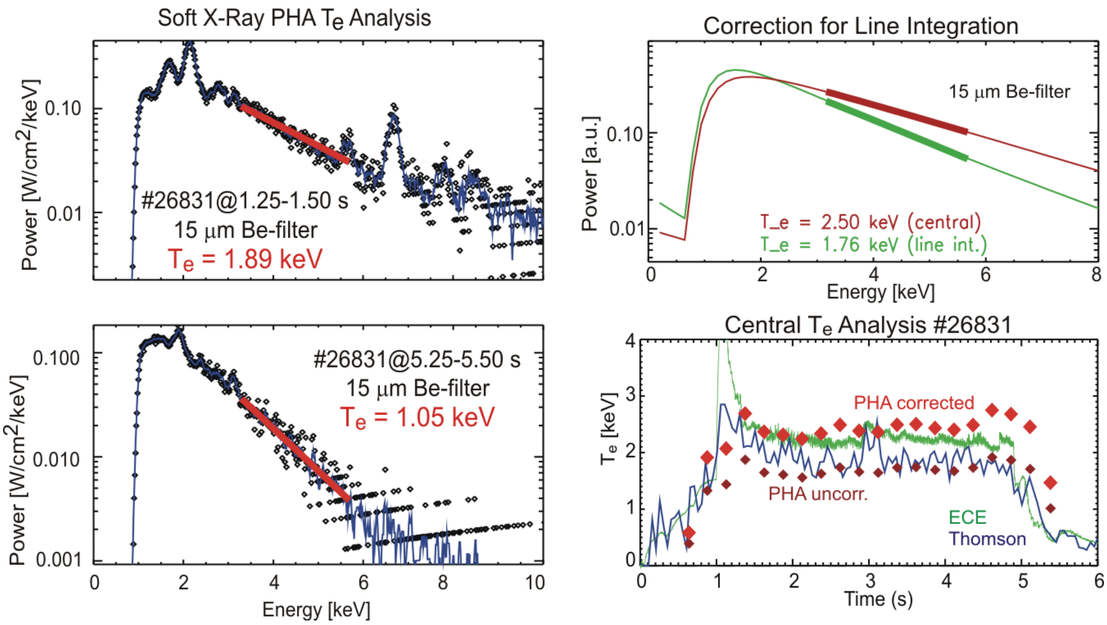

Fig. 4 Electron temperature from the slope of the continuous spectrum. Left: fitted curve (red) at 2 different times. Upper right: forward modeling of central and line integrated spectra yields correction factors to estimate central temperatures which are compared with other data (bottom).

Two extreme examples are shown in fig. 3, where measured PHA spectra are compared with spectra modelled by the IONEQ code [8], using T_e and n_e profiles from integrated data analysis [9]. In the first case the spectrum taken with a thin Be-filter (15 µm) is completely dominated by Argon, although the concentration is only about $2{\cdot}10^{-4}$. The standard analysis of data from the Johann spectrometer yields about 3 times higher values taking input profiles generated in a different way and using the more elaborate atomic dataset from ADAS. The second spectrum (1 mm Be-filter, right) yields an iron concentration of $2{\cdot}10^{-4}$, and shows again the high sensitivity of the PHA diagnostics for detecting small fractions of impurities.

The PHA data also contain information on T_e, which can be inferred from the slope of the continuous part of the spectra. An example of such an analysis is shown in fig. 4. The direct measurements are averages over the hot plasma core along the line of sight. In order to get estimates of the central electron temperature, correction factors were evaluated from forward modelling of the continuum radiation and comparing T_e from the analysis of the line integrated profiles with the central value of T_e used in the simulation. Thus, a reasonable agreement with other temperature measurements is achieved.

[1] R. Neu, et al. *Plasma Phys. Control. Fusion* **49**(12B) B59 (2007)
[2] T. Pütterich, et al. *Plasma Phys. Control. Fusion* **50**(8) 085016 (2008)
[3] W. Suttrop, *this conference* (2011)
[4] T. Pütterich, et al. *Nucl. Fusion* **50**(2) 025012 (2010)
[5] C. Biedermann, et al. *Phys. Scr.* **T134** 014026 (2009)
[6] R. Radtke, et al. *J. Phys.: Conf. Ser.* **58**(1) 113 (2007)
[7] R. Dux, et al. *Nucl. Fusion* **51**(5) 053002 (2011)
[8] A. Weller, et al. Modelling of soft X-ray emission from JET plasmas, Report JET-IR(87)10 (1987) (unpublished)
[9] R. Fischer, et al. *Fusion Science and Technology* **58**(2) 675-684 (2010)